Magnetization of $La_{2-x}Sr_xNiO_{4+\delta}$ ($0 \leqslant x \leqslant 0.5$): Spin-glass and memory effects

P. G. Freeman,* A. T. Boothroyd, and D. Prabhakaran
Department of Physics, Oxford University, Oxford OX1 3PU, United Kingdom

J. Lorenzana
SMC-INFM, ISC-CNR, Dipartimento di Fisica, Università di Roma La Sapienza, P. Aldo Moro 2, 00185 Roma, Italy
(Received 4 September 2005; revised manuscript received 20 December 2005; published 31 January 2006)

We have studied the magnetization of a series of spin-charge-ordered $La_{2-x}Sr_xNiO_{4+\delta}$ single crystals with $0 \leqslant x \leqslant 0.5$. For fields applied parallel to the *ab* plane there is a large irreversibility below a temperature $T_{F1} \sim 50$ K and a smaller irreversibility that persists up to near the charge-ordering temperature. We observed memory effects in the thermoremnant magnetization across the entire doping range. We found that these materials retain a memory of the temperature at which an external field was removed and that there is a pronounced increase in the thermoremnant magnetization when the system is warmed through a spin reorientation transition.

DOI: 10.1103/PhysRevB.73.014434 PACS number(s): 75.50.Lk, 75.30.Fv, 71.45.Lr, 75.60.Ej

I. INTRODUCTION

In the last decade it has become apparent that hole-doped antiferromagnetic oxides have a strong tendency to form complex ordered phases involving spin and charge degrees of freedom. Among the most studied such materials are the layered superconducting cuprates $La_{2-x}Sr_xCuO_4$ (LSCO) and the isostructural but nonsuperconducting nickelates $La_{2-x}Sr_xNiO_4$ (LSNO), both of which exhibit a spin-charge-ordered "stripe" phase.[1,2] Also common to the phase diagram of both these systems is a so-called "spin-glass" phase, identified from irreversible behavior in magnetization measurements.[3,4]

The close proximity of the stripe and spin glass phases suggest that these phenomena might be related. Evidence of the glassy nature of stripe phases has already been found in neutron diffraction measurements. Tranquada *et al.* studied the stripe-ordered phase of $La_{1.6-x}Nd_{0.4}Sr_xCuO_4$ with $x=0.12$ and $x=0.15$ and observed slowly fluctuating short-range magnetic correlations which persisted above the bulk magnetic-ordering temperature, indicating a glassy transition to the ordered state.[5] Similarly, diffraction measurements on LSNO have shown that neither the charge-ordering transition nor the magnetic-ordering transition are particularly well defined.[6–10] Further, a recent study of the bulk magnetization in superconducting LSCO found that the irreversible magnetization of LSCO behaves in a manner that resembles the fundamental properties of the superconducting state.[11] The possibility of a connection between stripes, spin-glass behavior, and superconductivity is clearly of great interest.

The origin of the irreversibility in LSNO and LSCO is not well understood. A straightforward explanation is that quenched disorder frustrates the magnetic interactions and produces a canonical spin glass.[3] The puzzling results of Ref. 11 in LSCO, however, suggest that superconducting correlations above T_c may be responsible for the irreversibility seen in that material.

The purpose of the present work was to investigate the relationship between irreversibility effects observed in magnetization measurements and the ordering properties of the stripe phase. We chose to study the LSNO system because stripe ordering extends over a wide range of doping and has been characterized in detail.[2,12–15] In addition, LSNO is not superconducting, so, in principle, it should help to distinguish irreversibility associated with charge and spin ordering alone from irreversibility associated also with superconductivity.

The basic stripe pattern in LSNO is illustrated in Fig. 1.[16] Holes introduced into Mott-insulating NiO_2 layers by Sr or O doping arrange themselves into an array of parallel lines in a background of antiferromagnetically ordered Ni^{2+} spins. The charge stripes, which are aligned at 45° to the Ni-O bonds, act as antiphase domain boundaries to the antiferromagnetic order. The stripe-ordering pattern that forms at $x=1/3$, shown in Fig. 1, is special because it is commensurate with the underlying square lattice of the NiO_2 plane with both the charge and magnetic order having the same period. This leads to a particularly stable ordering at this doping

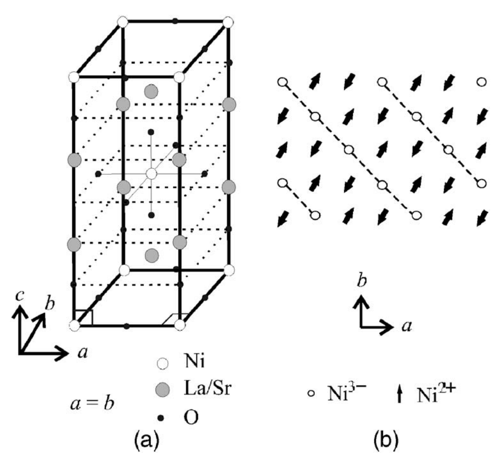

FIG. 1. (a) Tetragonal unit cell of $La_{2-x}Sr_xNiO_4$. (b) Pattern of spin-charge ordering in the NiO_2 planes in $La_{5/3}Sr_{1/3}NiO_4$. Arrows denote $S=1$ spins on the Ni^{2+} ions and open circles represent holes, here assumed centered on Ni sites. The dashed lines indicate the charge stripes. The O sites are not shown for clarity.

level.[12,17,18] At other doping levels the spin and charge order are incommensurate with the crystal lattice, and a model based on periodically spaced discommensurations has been proposed to explain the ordering wave vectors observed in diffraction experiments. There is some evidence that the charge stripes are located on the Ni sites, creating formally Ni^{3+} ions,[19] but there is also evidence that the holes can reside at least for some of the time in oxygen orbitals.[20] Spin degrees of freedom also exist within the charge stripes but these do not form long-range static magnetic order. There are, however, quasi-one-dimensional antiferromagnetic correlations between the spins in the charge stripes.[21]

The stripe-ordered phase has been observed in $La_{2-x}Sr_xNiO_4$ for Sr doping in the range $0.135 \leqslant x \leqslant 0.5$ and also in some oxygen-doped compounds $La_2NiO_{4+\delta}$.[6,8,10,12–17,22–26] Charge ordering occurs at a temperature T_{CO} typically 100–200 K depending on doping. Magnetic order occurs at a slightly lower temperature T_{SO}. An exception is $x=0.5$ which has an anomalously high charge-ordering temperature of $T_{CO} \simeq 480$ K due to the particular stability of the checkerboard charge-ordering pattern that forms at half doping.[2,14] Below $T_{IC} \approx 180$ K the checkerboard pattern becomes slightly incommensurate, and below $T_{SO} \simeq 80$ K it is accompanied by incommensurate magnetic order. The origin of these incommensurate effects is not well understood. The correlation lengths of the charge and stripe order in these materials are typically 100–300 Å for $0.2 < x \leqslant 0.47$ with both correlation lengths being particular long in commensurately ordered $x=1/3$.[12,26]

An interesting feature of the magnetic order in LSNO is the existence of a spin reorientation transition. This transition features strongly in the present work. It was first observed in the $x=1/3$ and $x=1/2$ materials at a temperature T_{SR} of 50 K and 57 K, respectively.[10,13] At the spin reorientation transition the spins, which lie in the *ab* plane at a nontrivial angle to the crystal axes, were observed to rotate within the *ab* plane through an angle of 13° ($x=1/3$) or 26° ($x=1/2$). Recently, a similar spin reorientation was found in $x=0.275$, 0.37 and $x=0.4$ compositions but at a reduced temperature of $\sim$15 K.[15]

In this work we studied the magnetization of a series of LSNO single crystals covering a wide range of doping levels. Our work complements a recent analysis of high-temperature magnetization described by Winkler *et al.*[27] A preliminary account of some of our results was given in Ref. 28, and here we describe our experiments in more detail. We observe irreversible magnetic behavior in all the samples for the case where the magnetic field was applied parallel to the *ab* plane. We also observed for this field orientation some interesting memory effects associated with the magnetic irreversibility.

II. EXPERIMENTAL DETAIL

Single crystals of $La_{2-x}Sr_xNiO_{4+\delta}$ with $0 \leqslant x \leqslant 0.5$ were grown in Oxford by the floating-zone technique.[29] Typical dimensions of the crystals used in this work were $\sim 5 \times 5 \times 2$ mm^3. The oxygen excess δ, determined by thermogravimetric analysis (TGA), is given for each crystal in Table I.

TABLE I. Oxygen excess δ of crystals of $La_{2-x}Sr_xNiO_{4+\delta}$ determined by thermogravimetric analysis. The nominal hole content n_h is given by $n_h=x+2\delta$.

x	δ (±0.01)	n_h (±0.02)
0	0.11	0.22
0.1	0.075	0.25
0.2	0.01	0.22
0.225	0.07	0.365
0.25	0.06	0.37
0.275	0.02	0.315
0.3	0.01	0.32
0.333	0.015	0.36
0.37		
0.4	0.005	0.41
0.5	0.02	0.54

Our results for the variation of δ with x are broadly consistent with a previous report for zone-melted crystals.[30] Crystals with $x \leqslant 0.25$ have significant excess oxygen, whereas those with $0.275 \leqslant x \leqslant 0.5$ are almost stoichiometric. The only exception is the crystal with $x=0.2$ which has an anomalously low value of δ. No TGA measurement was carried on the $x=0.37$ composition, but from Table I we would expect $\delta \simeq 0.01$ since this crystal was grown under similar conditions to the others. Moreover, the temperature dependence of the magnetic and charge order of crystals from the same batches as those studied here has previously been measured for most Sr compositions by neutron or x-ray diffraction.[10,15,25,26] The incommensurability of the $x=0.37$ crystal was found to be in line with that of the $x=0.333$ and $x=0.4$ crystals (see Fig. 4).

Magnetization measurements were carried out with a superconducting quantum interference device (SQUID) magnetometer (Quantum Design). The measurements were made by the dc method, with either the magnetic field parallel to the *ab* plane ($H \| ab$) or parallel to the crystal *c* axis ($H \| c$). For some of the measurements with $H \| c$ we used a rotating sample mount to align the crystal accurately via the anisotropy of the magnetization. The rotating mount contributes a significant magnetic background which had to be measured and subtracted from the signal. Any uncertainty in the subtraction will cause a systematic error in the magnetization, and so measurements taken with the rotating mount will be indicated.

Temperature scans of the magnetization were performed either by measuring while cooling the sample in an applied field of 500 Oe [field cooled (FC)] or by cooling the sample in zero field and subsequently measuring while warming in a field of 500 Oe [zero-field cooled (ZFC)]. Typically the data points were collected at a rate of one every 2–4 min. To study relaxation and memory effects we used several different field and temperature protocols which will be described later.

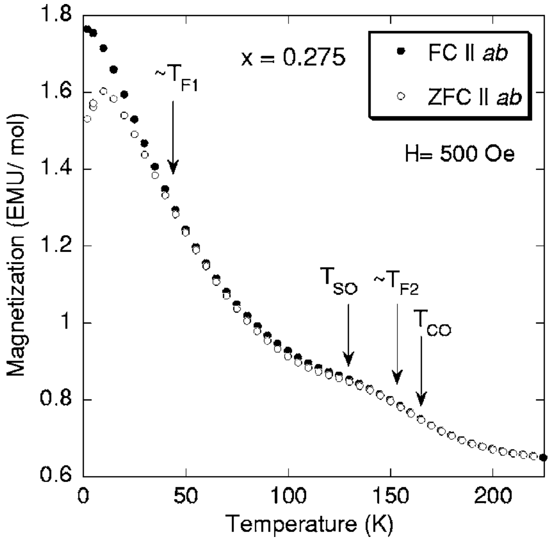

FIG. 2. Field-cooled (FC) and zero-field-cooled (ZFC) dc magnetization of $La_{1.725}Sr_{0.275}NiO_4$. The curves were measured with a field of 500 Oe applied parallel to the *ab* plane. T_{SO} and T_{CO} are the magnetic- and charge-ordering temperatures, respectively. The temperatures T_{F1} and T_{F2} are explained in the text.

III. RESULTS

A. Magnetization vs temperature

Figure 2 shows a typical set of results for the FC and ZFC magnetization of LSNO when the measuring field is applied parallel to the *ab* plane, in this case for a crystal with $x=0.275$. The FC and ZFC magnetization curves are seen to increase with decreasing temperature and follow one another closely, except at low temperature where there is a peak in the ZFC curve. We have indicated approximate charge- and magnetic-ordering temperatures T_{CO} and T_{SO} based on the temperature dependence of the charge and magnetic superlattice Bragg peaks measured by x-ray and neutron diffraction.[15,26] The charge and spin correlations build up rather slowly, over several tens of kelvin, so the ordering temperatures are not precisely defined. Nevertheless, charge ordering and magnetic ordering have quite distinct effects on the magnetization, as can be seen in Fig. 2. On cooling below T_{CO} the magnetization curve rises less steeply, but once the temperature drops below T_{SO} the curve begins to rise more rapidly again. This "wiggle" in the magnetization associated with T_{CO} and T_{SO} is observed for all samples with $x \geqslant 0.2$.

For most of the temperature range below T_{CO} the FC curve lies above the ZFC curve, indicative of glassy behavior. The FC-ZFC separation increases noticeably below the temperature marked $T_{F1} \approx 40$ K which is somewhat higher than the temperature at which the peak is observed in the ZFC curve. Above T_{F1} the FC-ZFC separation is approximately constant up to a temperature $T_{F2} \sim T_{CO}$, above which the FC and ZFC curves become coincident.

We carried out magnetization measurements on the 11 samples of $La_{2-x}Sr_xNiO_{4+\delta}$ listed in Table I. The results for several doping levels are presented in Fig. 3. The curves with $H \| ab$ all show similar features to those we have already described for the $x=0.275$ sample. In some cases there is an extra feature labeled T_{SR} associated with the spin reorientation transition.[10,13,15] This feature is especially prominent for the samples with $x=0.333$ ($T_{SR} \simeq 50$ K) and 0.5 ($T_{SR} \simeq 57$ K). For $x=0.37$ (Fig. 3) and 0.4 we observe the temperature T_{F2} to be higher than T_{CO}, whereas for the other compositions apart from $x=0.5$ we find T_{F2} to be similar to, or just below, T_{CO}. Our measurements on the $x=0.5$ sample did not extend high enough to reach the charge-ordering temperature of $T_{CO} \simeq 480$ K.[14]

For several of the samples (those with $x=0.2$, 0.3, 0.333, and 0.5) we measured magnetization curves with $H \| c$. In each case the curves with $H \| c$ lie below those with $H \| ab$, consistent with previous observations.[30] Interestingly, when $H \| c$ we observe little or no difference between the FC and ZFC magnetizations for these samples.

In Fig. 4 we plot the charge-ordering temperatures for our crystals determined either directly by x-ray diffraction or from the wiggle in the magnetization. For comparison we have included results for LSNO published by other groups.[8,12–14,17,22] We have not shown any data for our $x=0$ and $x=0.1$ crystals because although these are expected to exhibit charge ordering based on the total hole count $n_h=x+2\delta$, we did not examine these crystals by x-ray or neutron diffraction and there is no feature in the magnetization data that we can identify with a charge-ordering transition. Our results are reasonably consistent with the literature results. In the literature such phase diagrams are often plotted as a function of n_h rather than x on the assumption that as far as the spin- and charge-ordering temperatures are concerned oxygen doping is equivalent to Sr doping. This assumption does not appear to be valid for our samples. The inset to Fig. 4 showing T_{CO} against n_h for our samples does not have a smooth variation, whereas the main plot of T_{CO} against x does. An inequivalence between Sr doping and oxygen doping was also found in the magnetic-ordering temperatures of a large set of polycrystalline samples of LSNO by Jestädt *et al.* using muon spin resonance (μSR).[31]

The peak in the ZFC magnetization was found to occur at approximately the same temperature (~ 10 K) for most of the samples. The only exceptions are $x=0.1$, 0.2, and 0.5, for which the peak occurs at ~ 25 K. It is not clear why the peak should occur at a higher temperature in these particular compositions.

The observation of features in the magnetization of stripe-ordered LSNO indicative of spin-glass and spin-freezing behavior (the FC-ZFC difference and the peak in the ZFC magnetization) suggests that the system is out of thermodynamic equilibrium at low temperatures and that relaxation effects in the experimental time scale may be important. In fact, a time-dependent remnant signal was reported some time ago by Lander *et al.* for a crystal with $x=0.15$.[32] To investigate this effect in more detail we performed the following experiment. We applied a field of 500 Oe parallel to the *ab* plane at fixed temperature for 5 min, turned the field off, and measured the remnant magnetization as a function of time. Figure 5 shows the results for the $x=1/3$ crystal measured at 2 K. The remnant signal has an initial rapid decay on a time scale of ~ 1000 s followed by a much slower decay extending beyond the duration of our experiment (~ 7000 s). We

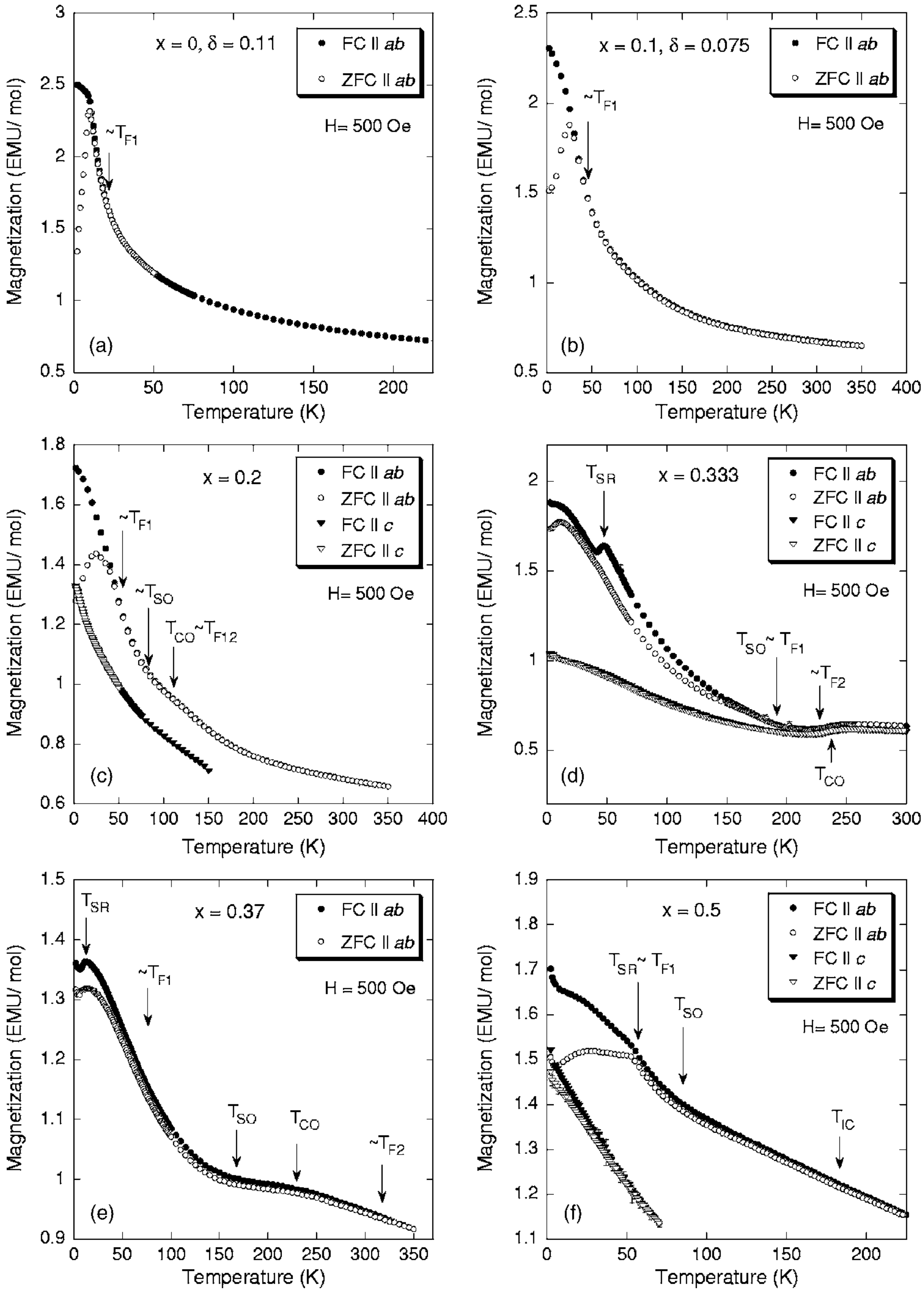

FIG. 3. Field-cooled (FC) and zero-field-cooled (ZFC) magnetization of single crystals of $La_{2-x}Sr_xNiO_{4+\delta}$ with $0 \leqslant x \leqslant 0.5$. A rotating sample mount was employed to obtain the data with $H \| c$ for the $x=0.333$ crystal.

attempted to fit the remnant signal with a stretched exponential $M(t)=M\exp\{-\alpha t^{(1-n)}\}$, as found to describe the magnetization in spin glasses,[33] but the quality of the best fit is not satisfactory, as can be seen in Fig. 5. This suggests that the mechanism by which the system decays back to equilibrium is not the same as in other spin glasses. Remnant magnetization is observed parallel to the *ab* plane for all temperatures below T_{F2} for all doping levels studied in this work.

B. Memory effects

The measurements presented so far indicate that the response of stripe-ordered LSNO to a magnetic field is partly irreversible, in the sense that application of a field followed by cooling to low temperatures creates a different state to cooling in zero field followed by application of a field, at least on the time scale of the measurement. As shown in Fig. 5, the magnetization is time dependent but the system does not reach a steady state at low temperature even after several hours.

In this section we describe a novel memory effect associated with the slow relaxation of the remnant magnetization. The first results we describe were obtained with the following field-temperature protocol: the sample is cooled from 300 K to a temperature T_0 in a field of 500 Oe applied parallel to the *ab* plane. Once at T_0 the field is removed, the sample is cooled to 2 K in zero field, and the thermoremnant

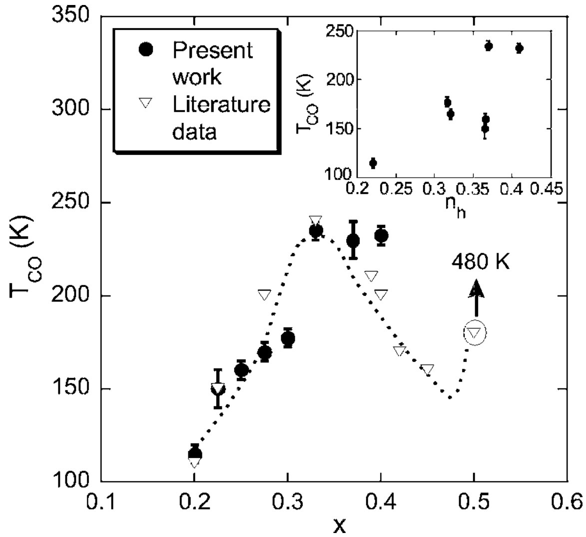

FIG. 4. Charge-ordering temperature of single crystals of $La_{2-x}Sr_xNiO_{4+\delta}$ as a function of Sr doping x. The inset shows the charge-ordering temperatures plotted against the effective hole concentration $n_h = x + 2\delta$; the error in n_h is ±0.02 due to the uncertainty in the oxygen content. Literature data are taken from Refs. 8, 12–14, 17, and 22.

magnetization (TRM) is measured while warming the sample up through T_0.

Figure 6(a) shows a typical TRM response obtained with this protocol. In this instance the data were obtained from the $x=0.2$ sample with $T_0=10$ K. On warming from 2 K the TRM is fairly constant up to T_0, but above T_0 it falls dramatically with increasing temperature. Hence, the system has a clear "memory" of the temperature at which the field was switched off.

The memory effect shown in Fig. 6(a) was observed for all the samples studied providing T_0 did not exceed T_{F2}. However, this is not the only interesting feature revealed by this measurement protocol. Figure 6(b) shows the TRM of samples with $x=0.333$ and $x=0.5$ using the same protocol, again with $T_0=10$ K. The memory effect at T_0 can clearly be seen, but there is also another dramatic feature in the curves, this time at a temperature in the region of 50 K. For $x=0.333$ this feature takes the form of a sharp upwards step in the curve, whereas for $x=0.5$ it is an abrupt change in slope. This second feature is not present in the data for $x=0.2$ shown in Fig. 6(a), and we associate it with the spin reorientations found near 50 K in $x=0.333$ and $x=0.5$ samples[10,13] (the $x=0.2$ sample does not have a spin reorientation near 50 K).

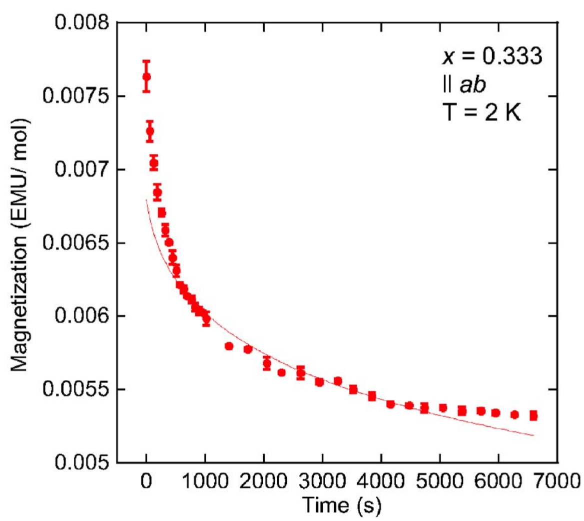

FIG. 5. (Color online) Time dependence of the remnant magnetization for a crystal of $La_{2-x}Sr_xNiO_4$ with $x=0.333$. The signal was induced by application of a magnetic field of strength 500 Oe parallel to the ab plane for 5 min at $T=2$ K. The time is measured after the field has been switched off. The curve is the best fit to a stretched exponential.

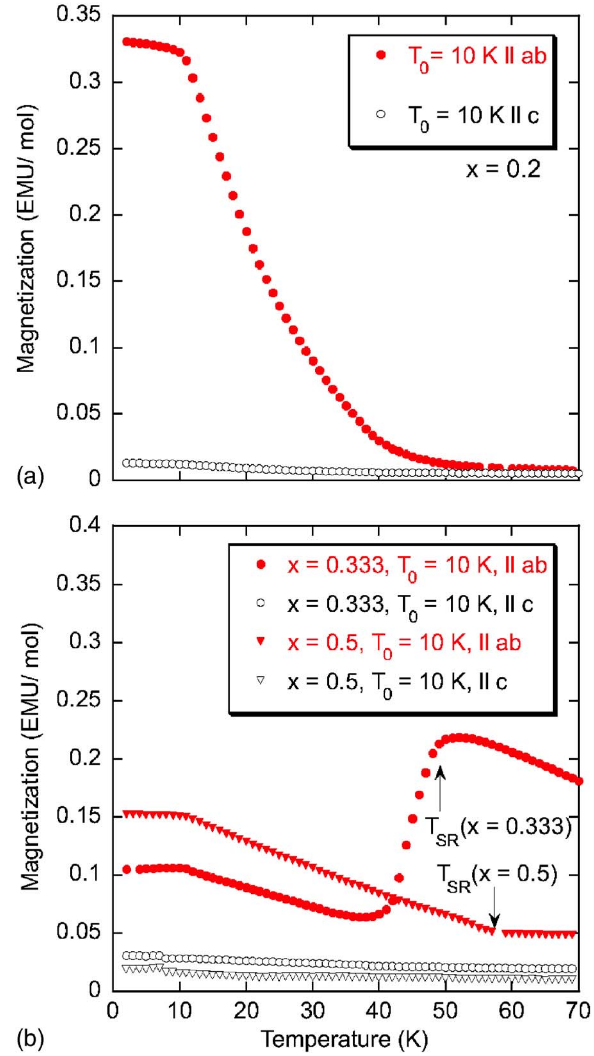

FIG. 6. (Color online) The thermoremnant magnetization (TRM) of $La_{2-x}Sr_xNiO_4$ induced by field cooling down to $T_0 = 10$ K in a field of 500 Oe followed by cooling to 2 K in zero field and measuring while warming in zero field. The symbols distinguish measurements made with the field applied parallel to the ab plane (solid symbols) and parallel to the c axis (open symbols). Panel (a) shows data for $x=0.2$, and panel (b) shows the corresponding measurements for the $x=0.333$ and $x=0.5$ samples, showing the striking effects associated with the spin reorientation transition (indicated by T_{SR}) in these two compositions. The rotating mount was used to obtain $H \parallel c$ data for the $x=0.333$ sample.

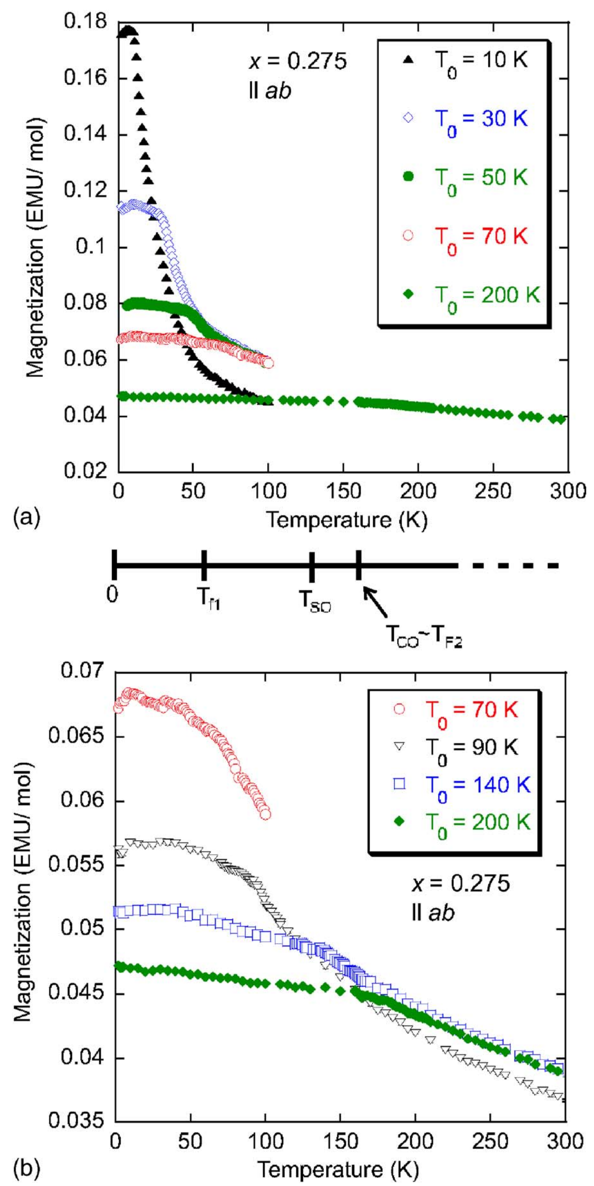

FIG. 7. (Color online) The TRM of LSNO, $x=0.275$, for different values of T_0, where T_0 is the temperature at which the magnetic field was switched off in the protocol described in the text and in the caption to Fig. 6. (a) shows data for $T_0=10$ K, 30 K, 50 K, 70 K, and 200 K, and (b) shows data for $T_0=70$ K, 90 K, 140 K, and 200 K.

In Figs. 7(a) and 7(b) we show results for the $x=0.275$ crystal for several different T_0 values. As T_0 increases the low-temperature TRM systematically decreases. For $T>T_0$ the curves tend to fall one on top of each other. Failure of the curve with $T_0=10$ K to do so could be due to fluctuations in the small residual field (~ few Oe) in the magnet.

The TRM signal continues to decay above the charge-ordering temperature $T_{CO}\simeq 160$ K. The anomaly at T_0 seems to be clearest when $T_0<T_{F1}$ (i.e., the runs with $T_0=10$ K, 30 K, and 50 K), but is still discernible in the runs with $T_0=70$ K, 90 K, and 140 K. There is no T_0 anomaly in the curve for $T_0=200$ K, but there is a change in slope in the region of T_{CO}. The $x=0.275$ composition is known to undergo a spin reorientation below $T_{SR}\simeq 12$ K,[15] and this may explain the initial slight increase in the TRM up to $\sim T_{SR}$.

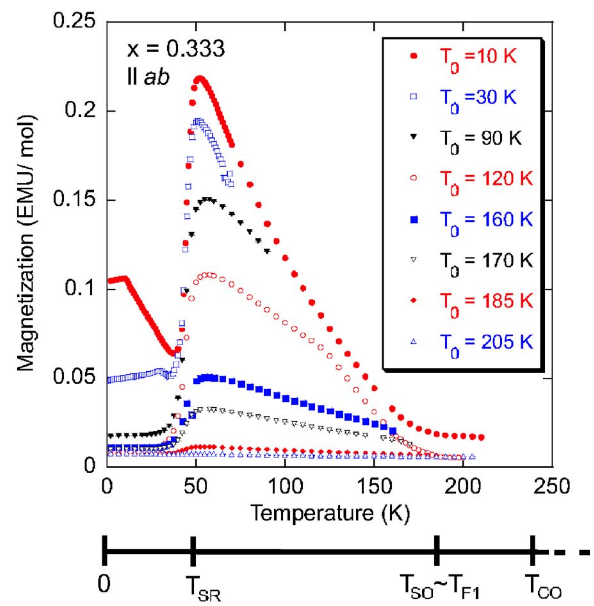

FIG. 8. (Color online) The TRM of LSNO, $x=0.333$, for different values of T_0, where T_0 is the temperature at which the magnetic field was switched off in the protocol described in the text and in the caption to Fig. 6.

Figure 8 displays the TRM of the $x=0.333$ sample for several different T_0 temperatures. All the curves apart from that for $T_0=205$ K rise sharply to a peak at a temperature close to $T_{SR}\simeq 50$ K. The smaller the value of T_0, the larger is the peak. The memory effect at T_0 is also present in these data, both when $T_0<T_{SR}$ and when $T_0>T_{SR}$ (see, for example, the curve for $T_0=120$ K) but not when $T_0>T_{F1}$ (e.g., $T_0=205$ K).

The memory effects at T_0 and T_{SR} just described are only observed when the field is applied parallel to the *ab* plane. As shown in Fig. 6, for fields parallel to the *c* axis the TRM is very small, and although there is a hint of a T_0 anomaly in the $x=0.2$ and $x=0.5$ curves, this could equally be the result of a misalignment of the *c* axis by a few degrees.

For some of the samples, we investigated the dependence of the TRM on several other parameters. We found that the remnant magnetization increased in size almost linearly with the inducing field, with little indication of saturation for inducing fields up to 5 T. We also found that the magnitude of the induced signal was the same for field-cooling rates from room temperature to T_0 of 10 K/min and 3 K/min.

Finally, Fig. 9 shows the TRM measured with the usual field-temperature protocol for two other LSNO samples. Both measurements were made with $T_0=10$ K. The T_0 anomaly is particularly strong in the sample with $x=0$ and $\delta=0.11$. This may be because for this sample T_0 coincides with a very sharp peak in the ZFC magnetization [Fig. 3(a)]. For the $x=0.37$ sample the signal around T_0 does not fall sharply like it does in the other samples, but this is probably because the T_0 anomaly is almost coincident with the memory signal associated with the spin reorientation which is known to occur below $T_{SR}=19$ K in this sample.[15]

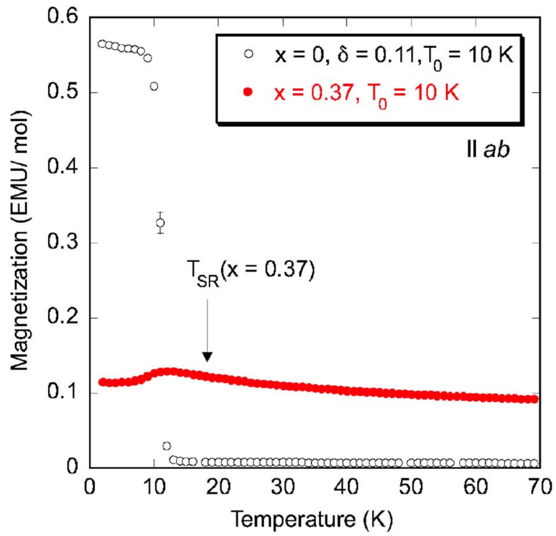

FIG. 9. (Color online) The TRM of samples of LSNO with $x=0$, $\delta=0.11$, and $x=0.37$. Here, $T_0=10$ K is the temperature at which the magnetic field was switched off in the protocol described in the text and in the caption to Fig. 6. The spin reorientation temperature T_{SR} of the $x=0.37$ sample is indicated.

IV. DISCUSSION AND CONCLUSIONS

The magnetization curves for the $La_{2-x}Sr_xNiO_{4+\delta}$ compounds reported here show a number of common features. For fields applied parallel to the *ab* plane there is a large irreversibility below a temperature T_{F1} and a smaller irreversibility that persists up to $T_{F2} \sim T_{CO}$ (Fig. 3). A peak is observed in the ZFC magnetization at temperatures in the range 10–30 K. This peak is generally rather rounded, reminiscent of a spin-glass-freezing transition. For the sample with $x=0$, $\delta=0.11$ the peak is much sharper, more like a transition to long-range magnetic order. On the other hand, the neutron diffraction study of Nakajima *et al.* on a crystal of nominally the same composition revealed a transition to long-range antiferromagnetic order at $T_N \simeq 50$ K rather than at 10 K.[34] The magnetization curves also exhibit features associated with spin reorientation transitions, identified here with the help of prior neutron diffraction results.

The fact that the irreversibility in the magnetization is only observed for fields parallel to the *ab* plane implies that it derives from the spins in the antiferromagnetic regions between the charge stripes (see Fig. 1). These spins have a small *XY*-like anisotropy, and in the magnetically ordered phase they line up parallel to the *ab* plane. It is then reasonable to assume that the irreversibility originates from some degree of disorder in the array of stripes, the disorder being either quenched or self-generated. Schmalian and Wolynes[38] have shown that stripe systems with competing interactions on different length scales (here the short-range magnetic exchange and long-range Coulomb interactions) can undergo a self-generated glass transition caused by the frustrated nature of the interactions. Also, since the stripes are charged, quenched disorder due to the dopants will frustrate the ideal periodic ordering of the stripes and produce a complex energy landscape. This stripe glass state would have a large number of metastable states separated by energy barriers. Slow relaxation between these states would lead to relaxation behavior, consistent with what we have observed here (Fig. 5).

Physically, disorder in the stripe phase could take a number of different forms. One source is magnetic frustration where a stripe ends. From diffraction measurements it is known that the stripes have a finite length.[12,25] At the end of a charge stripe there is magnetic frustration where two antiphase spin domains meet without the charged wall to stabilize the antiphase configuration. Another possibility is variations in the direction of the ordered magnetic moments. As noted above, there is magnetic irreversibility associated with the spin reorientation transitions that occur in some, if not all, striped LSNO compounds. The ordered moments lie in the *ab* plane, but in general do not point along a symmetry direction within the plane.[15] The system could therefore contain spatially separated domains in which the moments point along different equivalent directions and which could be unequally populated. There is, in addition, some experimental evidence for a distribution of moment directions,[39] which could lead to disorder. A third possibility is that the finite-sized stripe domains could carry a net moment and there could be frustrated free spins at boundaries between the stripe domains. Finally, there are the spin degrees of freedom within the charge stripes to consider. Because these are at antiphase boundaries, the mean-field coupling to the antiferromagnetic order is frustrated (Fig. 1). Although these spins do not exhibit static long-range order, there is evidence for short-range dynamic antiferromagnetic correlations among them,[21] and these correlations could at least in principle freeze into a glassy state at low temperatures. However, the dynamical susceptibility of these fluctuating spins is observed to be largest in the *c* direction,[21] and this is inconsistent with the magnetization effects described here which only occur when the field is parallel to the *ab* plane.

Magnetic irreversibility and spin-glass-like behavior with a similar phenomenology to that reported here is known in a number of related magnetic oxide systems close to metal insulator transitions, such as layered cuprates,[35] manganates,[36] and cobaltates.[37] These are often discussed in terms of mesoscopic phase separation of differently ordered ground states with similar energy. For example, in $La_{1-x}Sr_xCoO_3$ there is strong evidence for the existence of nanoscale ferromagnetic clusters embedded in a nonmagnetic background matrix, and the glassy behavior is understood to arise from frustrated interactions between these magnetic particles.[37] The case of the nickelates is somewhat different at the doping levels we have been studying in that there is no evidence for the sort of nanoscale spin-charge phase separation found in $La_{1-x}Sr_xCoO_3$. However, as noted above, disorder in the stripe phase of $La_{2-x}Sr_xNiO_{4+\delta}$ could create free spins at the boundaries of stripe-ordered domains, and the way in which these free spins interact could be analogous to the mechanism that causes glassy behavior in other doped magnetic oxides.

Let us now discuss the memory effects observed here. Aging and memory effects are typical characteristics of spin glasses,[40] but here we have used a new protocol and observed a phenomenologically different memory effect. We have found that stripe-ordered nickelates have a memory of the temperature at which an external field is removed and also have a memory of the state of the system at the spin reorientation transition.

Aging and memory effects in spin glasses can be understood qualitatively in terms of jumps between a large number of metastable states separated by energy barriers. Consider the decay in the remnant magnetization on removing the magnetic field at constant temperature shown in Fig. 5. After the field is switched off there is an initial phase in which the magnetization decreases rapidly, with the system crossing small energy barriers reversibly, but soon the system reaches a second phase in which the magnetization decays much more slowly. During this second phase, the system evolves via a series of "quakes"—i.e., large, irreversible, configurational rearrangements involving many spins, driven by extremal thermal fluctuations.[41] Each quake drives a region of the system from one metastable configuration into another one with lower energy. The time needed to overcome a barrier of size Δ is of order

$$t(\Delta) \sim \tau_0 \exp\left(\frac{\Delta}{k_B T}\right), \tag{1}$$

with τ_0 a microscopic time. In a glassy state barriers are broadly distributed. Barriers which satisfy $t(\Delta) \lesssim t_{\mathrm{expt}}$ will lead to relaxation in the experimental time scale t_{expt}. However, a significant fraction of the barriers will satisfy $t(\Delta) > t_{\mathrm{expt}}$, leading to slow or virtually zero relaxation in the experimental time scale. In addition as the temperature is lowered it is expected that the height of the barriers grows.[42] Hence, the decay in the magnetization eventually slows to a virtual standstill before the true equilibrium ground state can ever be reached.

Now consider the memory effect shown in Fig. 6(a). After the field is switched off at T_0 the induced magnetization decays as just described to a long-time metastable state where barriers with $t(\Delta) > t_{\mathrm{expt}}$ hold parts of the system with a nonzero out-of-equilibrium magnetization. On cooling, the amount of thermal energy available decreases and the barriers increase, trapping the system in the long-time state established at T_0. On reheating the sample the thermal fluctuations are insufficient to quake the system out of its deep energy minimum as long as the temperature remains below T_0. However, as soon as the temperature exceeds T_0 the decrease in the heights of the barriers and the increase in the thermal fluctuations allow new parts of the system to relax, decreasing the TRM further.

If this description is valid, then it should in theory be possible to perform a cooling-reheating excursion anywhere on the TRM curve at $T > T_0$ and after the excursion return to the same TRM curve. An experiment to test this prediction is presented in Fig. 10. The $x=0.2$ sample was used, and we followed the usual field-temperature protocol with $T_0 = 20$ K. As expected, the TRM shows an abrupt drop on warming through $T_0 = 20$ K. On reaching 30 K, however, we stopped warming, cooled back down to 20 K, and started warming again at the same rate, measuring the TRM continuously from 20 K up to 60 K. As can be seen in Fig. 10,

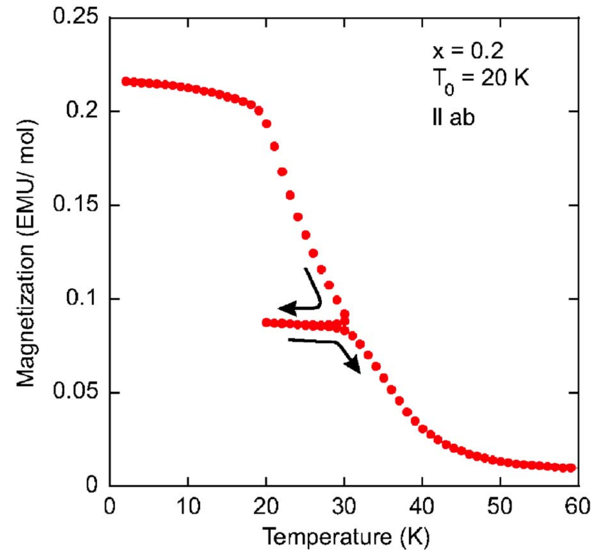

FIG. 10. (Color online) The TRM signal for the LSNO sample with $x=0.2$ resulting from the following protocol. First, the sample was cooled from room temperature to $T_0=20$ K in a field of 500 Oe applied parallel to the *ab* plane, the field removed, and the sample cooled to 2 K in zero field. The TRM was then measured while warming from 2 K to 30 K, then while cooling from 30 K to 20 K, and finally while warming from 20 K to 60 K.

during the temperature excursion from 30 K to 20 K and then back again to 30 K the TRM remains almost constant. On further warming the TRM returns to the original curve. This behavior is consistent with the picture we have described.

One of our comments about Fig. 7 was that the lower the temperature T_0, the larger the TRM. This is hardly surprising. First, the magnetization induced by the applied field increases with decreasing temperature (due, it must be assumed, to the existence of effective free spins associated with disorder), and second, at lower T_0 the thermal fluctuations are smaller and the barriers are higher, so more regions of the system contribute to the TRM. As already mentioned, we observe a large TRM for $T_0 < T_{F1}$ and a small TRM for $T_{F1} < T_0 < T_{F2} \sim T_{CO}$. This is evidence that the cause of the TRM is the same as that of the irreversible magnetization in the FC-ZFC protocol.

Perhaps the most dramatic effect we have observed is the remarkable increase in the TRM at the spin reorientation transition of the $x=0.333$ sample (see Fig. 8). Usually, TRM effects are characterized by a reduction in remnant magnetization with increasing temperature, whereas here we observe an increase of up to one order of magnitude. This is especially surprising given that the FC magnetization exhibits only a small drop on cooling through T_{SR} [Fig. 3(d)]. Memory effects have been observed in a number of different systems,[36,37,43] but unlike those systems, the LSNO compounds studied here exhibit a memory effect associated with a spin reorientation transition. To some extent the memory effects reported here are simpler than the phenomena reported in other glassy system in that our protocol does not involve a waiting time where the system ages. Rather, it depends on the cooling and heating protocol at relatively fast rates.

In summary, we have observed irreversible behavior and memory effects in the magnetization of $La_{2-x}Sr_xNiO_{4+\delta}$ when the magnetic field is applied parallel to the *ab* plane. We found particularly striking memory effects associated with a spin reorientation transition. These observations suggest that stripe-ordered LSNO has nontrivial dynamics, and it would be of interest to find out if similar effects were present in other stripe-ordered systems.

ACKNOWLEDGMENTS

We would like to acknowledge P. Isla and D. González of Instituto de Ciencia de Materials de Aragón, CSIC-Universidad de Zaragoza, Spain, for carrying out the thermogravimetric analysis of the crystals used in this work. We would also like to acknowledge that this work was supported in part by the Engineering and Physical Sciences Research Council of Great Britain. J.L. is indebted to F. Ricci-Tersenghi for enlightening discussions on memory effects.

*URL: http://xray.physics.ox.ac.uk/Boothroyd

[1] J. M. Tranquada, B. J. Sternleib, J. D. Axe, Y. Nakamura, and S. Uchida, Nature (London) **375**, 561 (1995); J. M. Tranquada, J. D. Axe, N. Ichikawa, Y. Nakamura, S. Uchida, and B. Nachumi, Phys. Rev. B **54**, 7489 (1996).

[2] C. H. Chen, S.-W. Cheong, and A. S. Cooper, Phys. Rev. Lett. **71**, 2461 (1993).

[3] M. Kato, Y. Maeno, and T. Fujita, J. Phys. Soc. Jpn. **60**, 1994 (1991); W.-J. Jang and H. Takei, Jpn. J. Appl. Phys., Part 1 **30**, 251 (1991); G. H. Lander, P. J. Brown, C. Stassis, P. Gopalan, J. Spalek, and G. Honig, Phys. Rev. B **43**, 448 (1991); Th. Strangfeld, K. Westerhold, and H. Bach, Physica C **183**, 1 (1991); S.-W. Cheong, H. Y. Hwang, C. H. Chen, B. Batlogg, L. W. Rupp, Jr., and S. A. Carter, Phys. Rev. B **49**, 7088 (1994).

[4] F. C. Chou, N. R. Belk, M. A. Kastner, R. J. Birgeneau, and Amnon Aharony, Phys. Rev. Lett. **75**, 2204 (1995).

[5] J. M. Tranquada, N. Ichikawa, and S. Uchida, Phys. Rev. B **59**, 14712 (1999).

[6] C.-H. Du, M. E. Ghazi, Y. Su, I. Pape, P. D. Hatton, S. D. Brown, W. G. Stirling, M. J. Cooper, and S.-W. Cheong, Phys. Rev. Lett. **84**, 3911 (2000).

[7] C. Hess, B. Buchner, M. Hucker, R. Gross, and S.-W. Cheong, Phys. Rev. B **59**, R10397 (1999).

[8] S.-H. Lee and S.-W. Cheong, Phys. Rev. Lett. **79**, 2514 (1997).

[9] K. Yamamoto, T. Katsufuji, T. Tanabe, and Y. Tokura, Phys. Rev. Lett. **80**, 1493 (1998).

[10] P. G. Freeman, A. T. Boothroyd, D. Prabhakaran, D. González, and M. Enderle, Phys. Rev. B **66**, 212405 (2002).

[11] C. Panagopoulos, M. Majoros, and A. P. Petrovic, Phys. Rev. B **69**, 144508 (2004).

[12] H. Yoshizawa, T. Kakeshita, R. Kajimoto, T. Tanabe, T. Katsufuji, and Y. Tokura, Phys. Rev. B **61**, R854 (2000); Physica B **241-243**, 880 (1998).

[13] S.-H. Lee, S.-W. Cheong, K. Yamada, and C. F. Majkrzak, Phys. Rev. B **63**, 060405(R) (2001).

[14] R. Kajimoto, K. Ishizaka, H. Yoshizawa, and Y. Tokura, Phys. Rev. B **67**, 014511 (2003).

[15] P. G. Freeman, A. T. Boothroyd, D. Prabhakaran, M. Enderle, and C. Niedermayer, Phys. Rev. B **70**, 024413 (2004).

[16] J. M. Tranquada, D. J. Buttrey, and D. E. Rice, Phys. Rev. Lett. **70**, 445 (1993).

[17] R. Kajimoto, T. Kakeshita, H. Yoshizawa, T. Tanabe, T. Katsufuji, and Y. Tokura, Phys. Rev. B **64**, 144432 (2001).

[18] A. P. Ramirez, P. L. Gammel, S.-W. Cheong, D. J. Bishop, and P. Chandra, Phys. Rev. Lett. **76**, 447 (1996).

[19] Jianqi Li, Yimei Zhu, J. M. Tranquada, K. Yamada, and D. J. Buttrey, Phys. Rev. B **67**, 012404 (2003).

[20] C. Schuessler-Langeheine, J. Schlappa, A. Tanaka, Z. Hu, C. F. Chang, E. Schierle, M. Benomar, H. Ott, E. Weschke, G. Kaindl, O. Friedt, G. A. Sawatzky, H.-J. Lin, C. T. Chen, M. Braden, and L. H. Tjeng, Phys. Rev. Lett. **95**, 156402 (2005).

[21] A. T. Boothroyd, P. G. Freeman, D. Prabhakaran, A. Hiess, M. Enderle, J. Kulda, and F. Altorfer, Phys. Rev. Lett. **91**, 257201 (2003).

[22] S. M. Hayden, G. H. Lander, J. Zarestky, P. J. Brown, C. Stassis, P. Metcalf, and J. M. Honig, Phys. Rev. Lett. **68**, 1061 (1992); V. Sachan, D. J. Buttrey, J. M. Tranquada, J. E. Lorenzo, and G. Shirane, Phys. Rev. B **51**, 12742 (1995); J. M. Tranquada, D. J. Buttrey, and V. Sachan, *ibid.* **54**, 12318 (1996).

[23] E. D. Isaacs, G. Aeppli, P. Zschack, S.-W. Cheong, H. Williams, and D. J. Buttrey, Phys. Rev. Lett. **72**, 3421 (1994); A. Vigliante, M. von Zimmermann, J. R. Schneider, T. Frello, N. H. Andersen, J. Madsen, D. J. Buttrey, Doon Gibbs, and J. M. Tranquada, Phys. Rev. B **56**, 8248 (1997).

[24] Yu. G. Pashkevich, V. A. Blinkin, V. P. Gnezdilov, V. V. Tsapenko, V. V. Eremenko, P. Lemmens, M. Fischer, M. Grove, G. Guntherodt, L. Degiorgi, P. Wachter, J. M. Tranquada, and D. J. Buttrey, Phys. Rev. Lett. **84**, 3919 (2000).

[25] P. D. Hatton, M. E. Ghazi, S. B. Wilkins, P. D. Spencer, D. Mannix, T. d'Almeida, D. Prabhakaran, A. Boothroyd, and S.-W. Cheong, Physica B **318**, 289 (2002).

[26] M. E. Ghazi, P. D. Spencer, S. B. Wilkins, P. D. Hatton, D. Mannix, D. Prabhakaran, A. T. Boothroyd, and S.-W. Cheong, Phys. Rev. B **70**, 144507 (2004).

[27] E. Winkler, F. Rivadulla, J.-S. Zhou, and J. B. Goodenough, Phys. Rev. B **66**, 094418 (2002).

[28] P. G. Freeman, A. T. Boothroyd, D. Prabhakaran, and D. Gonzalez, J. Magn. Magn. Mater. **272-276**, 958 (2004).

[29] D. Prabhakaran, P. Isla, and A. T. Boothroyd, J. Cryst. Growth **237**, 815 (2002).

[30] W.-J. Jang and H. Takei, Jpn. J. Appl. Phys., Part 1 **30**, 251 (1991).

[31] Th. Jestädt, K. H. Chow, S. J. Blundell, W. Hayes, F. L. Pratt, B. W. Lovett, M. A. Green, J. E. Millburn, and M. J. Rosseinsky, Phys. Rev. B **59**, 3775 (1999).

[32] G. H. Lander, P. J. Brown, C. Stassis, P. Gopalan, J. Spalek, and G. Honig, Phys. Rev. B **43**, 448 (1991).

[33] M. A. Continentino and A. P. Malozemoff, Phys. Rev. B **33**, 3591

(1986).
[34] K. Nakajima, Y. Endoh, S. Hosoya, J. Wada, D. Welz, H.-M. Mayer, H.-A. Graf, and M. Steiner, J. Phys. Soc. Jpn. **66**, 809 (1997).
[35] C. Panagopoulos and V. Dobrosavljevic, Phys. Rev. B **72**, 014536 (2005).
[36] F. Rivadulla, M. A. Lopez-Quintela, and J. Rivas, Phys. Rev. Lett. **93**, 167206 (2004).
[37] J. Wu, J. W. Lynn, C. J. Glinka, J. Burley, H. Zheng, J. F. Mitchell, and C. Leighton, Phys. Rev. Lett. **94**, 037201 (2005).
[38] J. Schmalian and P. G. Wolynes, Phys. Rev. Lett. **85**, 836 (1997).
[39] Y. Yoshinari, P. C. Hammel, and S.-W. Cheong, Phys. Rev. Lett. **82**, 3536 (1999).
[40] K. Jonason, E. Vincent, J. Hammann, J. P. Bouchaud, and P. Nordblad, Phys. Rev. Lett. **81**, 3243 (1998).
[41] P. Sibani and H. J. Jensen, JSTAT P10013 (2004).
[42] J.-P. Bouchaud, V. Dupuis, J. Hammann, and E. Vincent, Phys. Rev. B **65**, 024439 (2002).
[43] M. Sasaki, P. E. Jönsson, H. Takayama, and H. Mamiya, Phys. Rev. B **71**, 104405 (2005), and references therein.